Review paper

Cite as: Sahu AK, Kataria S, Gandikota G: Added value of high-resolution ultrasound and MRI in the evaluation of rheumatologic diseases. J Ultrason 2023; 23: e285–e298. doi: 10.15557/JoU.2023.0035.

Submitted: 22.09.2023
Accepted: 16.10.2023
Published: 30.10.2023

Added value of high-resolution ultrasound and MRI in the evaluation of rheumatologic diseases

Amit Kumar Sahu[1], Shweta Kataria[2], Girish Gandikota[2]

[1] Department of Radiology, Max Superspeciality Hospital, New Delhi, India
[2] Department of Radiology, University of North Carolina, Chapel Hill, USA

Corresponding author: Girish Gandikota; e-mail: gandikotag@gmail.com

DOI: 10.15557/JoU.2023.0035

Keywords
ultrasound; MRI; inflammatory arthritis; rheumatoid arthritis; psoriatic arthritis

Abstract

Rheumatologic diseases are a widespread group of disorders affecting the joints, bones, and connective tissue, and leading to significant disability. Imaging is an indispensable component in diagnosing, assessing, monitoring, and managing these disorders, providing information about the structural and functional alterations occurring within the affected joints and tissues. This review article aims to compare the utility, specific clinical applications, advantages, and limitations of high-resolution ultrasound and magnetic resonance imaging in the context of rheumatologic diseases. It also provides insights into the imaging features of various types of inflammatory arthritis with clinical relevance and a focus on high-resolution ultrasound and magnetic resonance imaging. By understanding the comparative aspects of high-resolution ultrasound and magnetic resonance imaging, it is easier for the treating physicians to make informed decisions when selecting the optimal imaging modality for specific diagnostic purposes, effective treatment planning, and improve patient outcomes. The patterns of soft tissue and joint involvement; bony erosion and synovitis help in differentiating between various type of arthritis. Involvement of various small joints of the hands also gives an insight into the type of arthritis. We also briefly discuss the potential applications of emerging techniques, such as ultrasound elastography, contrast-enhanced ultrasound, and dual-energy CT, in the field of rheumatology.

Introduction

Rheumatologic diseases are a heterogeneous group of disorders affecting the joints, muscles, bones, tendons, ligaments, and cartilage. Some of the most commonly known rheumatologic conditions include osteoarthritis, rheumatoid arthritis, gout, juvenile idiopathic arthritis, ankylosing spondylitis, systemic lupus erythematosus (SLE), polymyalgia rheumatica, Sjögren's syndrome, psoriatic arthritis, systemic sclerosis, vasculitis, and fibromyalgia. These diseases are typically chronic and can cause pain, inflammation, stiffness, and impaired function. This can lead to morbidity and work disability with significant socio-economic impact. A report by the CDC states that during 2016–2018, about 58.5 million (23.7%) US adults had arthritis and about 43.9% of them had arthritis-attributable activity limitations[(1)]. An estimated 78 million (26%) US adults are projected to have arthritis by the year 2040[(2)].

Clinical examinations can have limitations in terms of subjectivity and lack of sensitivity in the detection of early signs of rheumatologic diseases. Hence, imaging plays a crucial role in the diagnosis, treatment response, and management of rheumatologic disorders.

Radiographs are typically the initial imaging modality for evaluating joint and osseous damage. They reveal joint space narrowing, joint subluxation, bone erosions, osteophytes, and osteopenia. However, these changes occur late in the disease process, hence the need for other imaging modalities to help with early diagnosis.

High-resolution US (HRUS) and magnetic resonance imaging (MRI) are useful in detecting early symptoms of inflammation, erosions, synovitis, and other disease-specific alterations, allowing treatment to be initiated earlier, and thus improving patient outcomes, and establishing remission. They allow an objective and quantitative evaluation of disease activity, such as synovial thickness and vascularity, as well as quantifying joint damage. HRUS has the advantage of being a portable, widely accessible, low-cost real-time imaging modality with dynamic capabilities and high spatial resolution. Lack of radiation, ability to image multiple sites at once and compare bilateral joints, intervention guidance, and point-of-care application allowing quick correlation between clinical and imaging findings are just a few of the advantages that have made US so popular in rheumatology practice. Recent US advancements, such as high-resolution images, power Doppler, elastography, contrast-

enhanced US, and microvascular imaging, broaden the scope of its applications. High-resolution US presents hurdles in terms of deeper penetration, difficulties with identifying intraosseous lesions, operator dependency, and reproducibility.

MRI, with its superior soft tissue contrast, provides a detailed examination of the internal structure of bones and joints including the identification of bone marrow edema. However, its use is limited by restricted availability, longer scanning time, higher cost, and in some cases patient claustrophobia.

High-resolution US in rheumatology

US examinations in rheumatology are optimally performed by high-frequency (10–18 MHz) linear array transducers. High frequency translates to better image resolution but limited penetration. The "hockey stick" transducer with a smaller footprint proves valuable when assessing small joints and curved anatomy. The joints are assessed in longitudinal and transverse planes.

US can detect features of inflammation like synovial hypertrophy, tenosynovitis, vascularity, effusion, enthesitis, and bone erosions – sometimes even before the disease becomes clinically evident (Tab. 1). An increase in vascularity in the synovium of the joint, bursa, or tendon sheath has a direct correlation with inflammatory activity. Color Doppler (CD) and power Doppler (PD) US are used to identify increased vascularity.

US elastography can assess the stiffness of soft tissues, which may be altered in the acute inflammation phase, recovery phase, and the late phase of scarring.

Tab. 1. Features of rheumatologic diseases on HRUS

Disease	Joint involvement	Key features on HRUS
Degenerative		
Osteoarthritis (OA)	Knee Hand (1st CMC, DIP, PIP) Hip	Cartilage thinning and irregularity Intrasubstance echogenicity in cartilage Marginal Osteophytes Joint space narrowing Effusion Synovitis Medial meniscal extrusion
Inflammatory		
Rheumatoid arthritis (RA)	MCP PIP Wrist MTP	Synovitis Effusion Erosions Tenosynovitis Bursitis Enthesitis Tendinitis Rheumatoid nodules
Juvenile idiopathic arthritis	Knee Ankle Hand Elbow Hip	Synovitis Tenosynovitis Cartilage loss Enthesitis Bursitis Tendinitis
Lupus arthritis	MCP PIP Wrist	Synovitis Tenosynovitis
Spondyloarthropathies (SpA)	Hand Knees Wrist	Enthesitis Synovitis Tenosynovitis Bursitis Paratenonitis Dactylitis
Polymyalgia rheumatica (PMR)	Shoulder Hip	Bursitis Effusion
Crystal deposition diseases		
Gout	1st MTP Tarsal Ankle Knee	Double contour sign Tophi Erosions Synovitis Effusion
Pseudogout	Knee Wrist Ankle	Intracartilaginous echogenic crystal deposits Synovitis Effusion Enthesitis

Some of the limitations of the US include operator dependency, inability to assess deeper anatomy, inability to visualize bone marrow, and low specificity in distinguishing between different types of rheumatic disorders.

Magnetic resonance imaging (MRI) in rheumatology

The main indications for MRI include early detection of inflammation, confirmation of active changes and structural lesions, disease follow-up and therapy monitoring, and identification of complications.

MRI allows for the assessment of various areas that are inaccessible to US, including sacroiliac joints and intervertebral joints. It can aid in the detection of active inflammatory lesions, such as synovitis and bone marrow edema, which are pre-erosive lesions and can determine prognosis.

The routine sequences of MRI scanning for musculoskeletal applications include T1, Short tau inversion recovery (STIR), T2 sequence with fat suppression (T2FS), post-contrast T1 sequence with or without fat suppression, and proton-density fat suppression (PDFS) sequences.

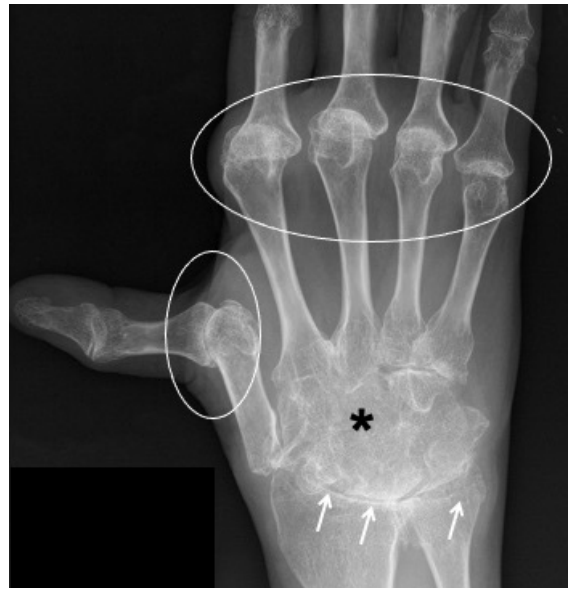

Fig. 1. *Rheumatoid arthritis (RA): AP radiograph of the hand demonstrates periarticular osteopenia (reduced bone density around the joints); reduced radiocarpal and intercarpal joint spaces; erosions (arrows), and subluxation of the metacarpophalangeal joints (white circles). Ankylosis of the intercarpal joints (asterisk) is seen in this case, which can be a feature of chronic untreated rheumatoid arthritis*

Rheumatoid arthritis (RA)

RA is a chronic autoimmune disorder of unknown etiology, but several genetic and environmental factors have been implicated in causation. The disease is characterized by synovial inflammation leading to the proliferation of synovium, also known as pannus, which if left untreated can eventually cause joint destruction and disability. With the advances in US and MRI, early diagnosis is possible, and therapy with newer, more effective disease-modifying anti-rheumatic drugs can be initiated to achieve remission before irreversible damage occurs. RA involves the proximal joints of the hand (wrist, metacarpophalangeal (MCP), and proximal interphalangeal joints (PIP)) and feet (midfoot, metatarsophalangeal (MTP), and proximal interphalangeal joints (PIP)). The involvement is usually bilateral and symmetric.

Conventional radiographs are usually the first-line imaging modality for RA. Features seen on radiographs include periarticular osteopenia, symmetrical joint space narrowing, marginal erosions, and soft tissue swelling (Fig. 1). In the early stages, the radiographs appear normal and thus, in the revised 2010 ACR/ EULAR diagnostic criteria, radiographic erosions are not included, as they represent a late stage in the disease course. US and MRI are more sensitive than radiographs and clinical examination in the early detection of disease[3], as pre-erosive synovitis can be seen in both modalities.

Synovitis

Synovial hypertrophy (SH) in US is defined as abnormal hypoechoic (relative to subdermal fat, but sometimes isoechoic or hyperechoic) intraarticular tissue that is non-displaceable and poorly compressible[4] (Fig. 2). These features help in differentiating synovial hypertrophy from joint effusion (Fig. 3).

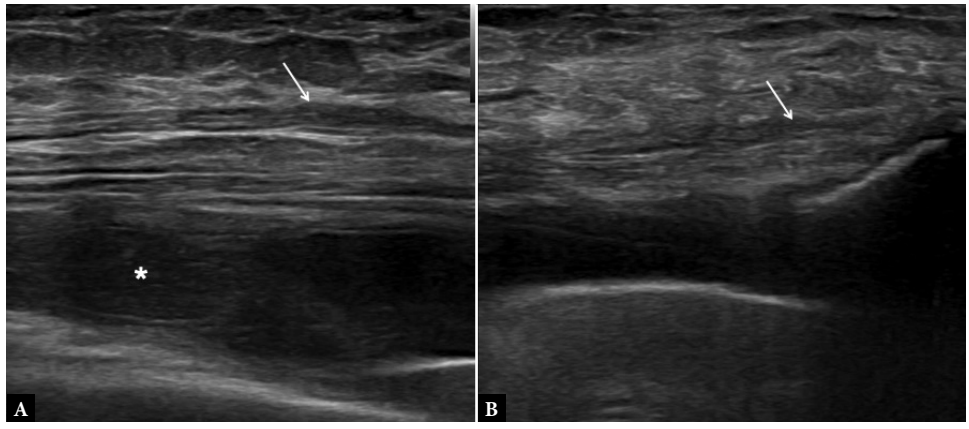

Fig. 2. *Synovitis. Long-axis US image of the suprapatellar knee showing echogenic synovium (asterisk in* **A***) which is partially compressible on probe pressure, as seen in image* **B**. *Arrows indicate the quadriceps tendon*

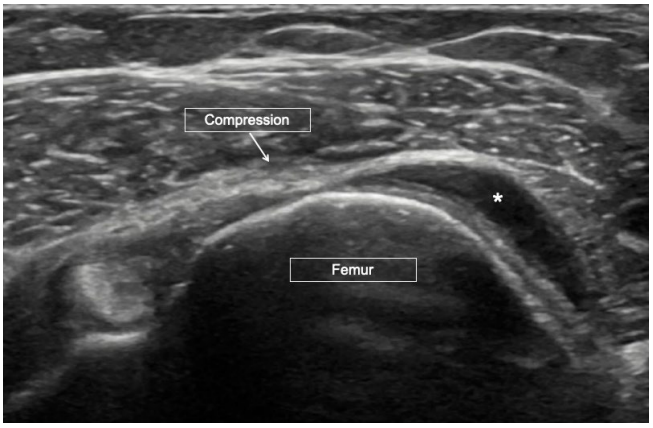

Fig. 3. *Joint effusion. Short-axis US image of the shoulder joint with absent rotator cuff. Central compression (arrow) shows complete compression and displacement of the joint fluid (asterisk)*

Synovitis is diagnosed when synovial hypertrophy exhibits signal on color flow Doppler interrogation (Fig. 4). PD is considered more sensitive than CD in identifying and quantifying increased vascularity and can be used to monitor disease activity and treatment response[5]. Szkudlarek *et al.*[6] developed a semiquantitative grading of the PD evaluation of synovitis: grade 0 – no flow; grade 1 – single-vessel signals; grade 2 – less than half of the area of the synovium-filled with vessels; grade 3 – more than half of the area of the synovium filled with vessels (Fig. 5).

A EULAR-OMERACT combined scoring system for grading synovitis in rheumatoid arthritis was proposed in 2017[7] (Tab. 2).

Researchers assessed the inter- and intraobserver reliability and concluded that the EULAR-OMERACT score demonstrated moderate-good reliability in MCP joints using a standardized scan and was equally applicable to non-MCP joints[8].

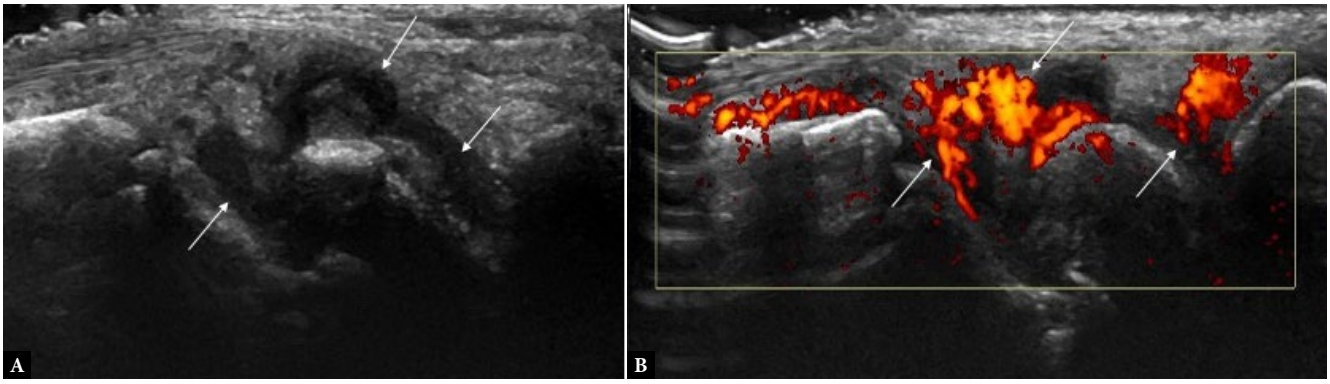

Fig. 4. *Greyscale (***A***) and power Doppler (***B***) long-axis US images of wrist joint depicting hypoechoic synovial proliferation (arrows in* **A***) distending the joint capsule with diffuse vascularity (arrows in* **B***)*

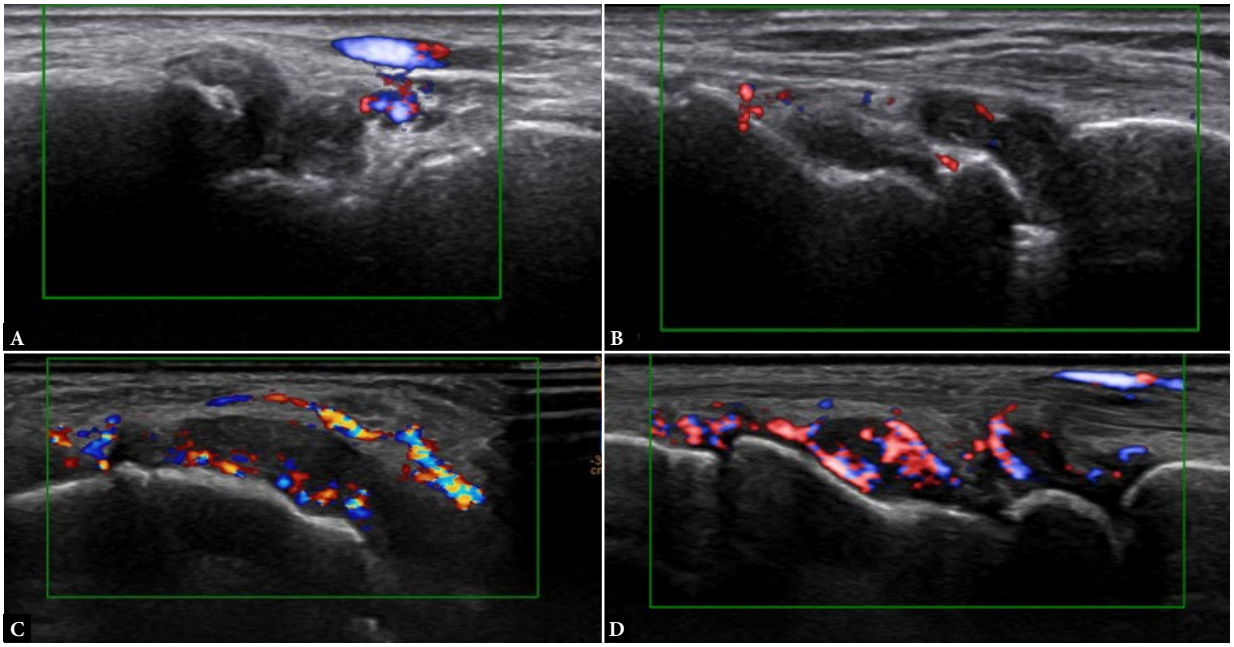

Fig. 5. *Power Doppler synovitis grading. Long-axis PDUS of the wrist joint shows grade 0 –no flow (***A***); grade 1 – single-vessel signal (***B***); grade 2 – less than half of the area of the synovium-filled with vessels (***C***); grade 3 – more than half of the area of the synovium filled with vessels (***D***). Note: the Doppler signal in (***A***) is from the periarticular vessels and not the synovium*

Tab. 2. EULAR-OMERACT combined scoring system for grading synovitis in rheumatoid arthritis

Grade 0	Normal joint	No GS-detected SH and no PD signal (within the synovium)
Grade 1	Minimal Synovitis	Grade 1 SH and ≤ Grade 1 PD signal
Grade 2	Moderate Synovitis	Grade 2 SH and ≤ Grade 2 PD signal or Grade 1 SH and Grade 2 PD signal
Grade 3	Severe Synovitis	Grade 3 SH and ≤ Grade 3 PD signal or Grade 1 or 2 SH and Grade 3 PD signal
GS – grayscale; SH – synovial hypertrophy; PD – power Doppler		

On MRI, SH appears as thickened synovium, and it is hyperintense on T2-weighted images, which makes it difficult to differentiate it from effusion. Consequently, contrast administration can be useful to distinguish enhancing synovium from non-enhancing effusion (Fig. 6). Synovial enhancement should be examined within 10 minutes from contrast administration, after which the contrast agent diffuses into the synovial fluid[9]. MRI can be used to quantify synovial volume, which has been shown to correlate with disease activity[10].

Dynamic contrast-enhanced (DCE) MRI can assess the rate of contrast uptake by the inflamed synovium and help monitor disease activity and treatment response.

Some studies have found that US is less sensitive than MRI in the early detection of synovitis and tenosynovitis, but highly specific[11].

In a systematic review and meta-analysis, Takase-Minegishi *et al.*[12] compared the accuracy of US-detected synovitis versus MRI in the wrist, MCP, PIP, and knee joints, and found good agreement of US and MRI for detecting synovitis in the MCP and PIP joints, lower agreement for the wrist, and low agreement for the knee joint[12,13]. They concluded that US seemed to be a valid and reproducible technique for detecting synovitis in the wrist and finger joints. PD US showed better overall diagnostic accuracy than grayscale US.

Erosions

Chronic synovitis leads to periarticular bone resorption which forms bone erosions. The presence of bone erosions at the time of RA diagnosis is a poor long-term prognostic indicator. On US, erosions appear as an intraarticular discontinuity in the cortical bone surface identified on two orthogonal planes (Fig. 7). A study by Wakefield *et al.*[14] demonstrated that US was more sensitive in the detection of erosions than radiography, especially in early disease. In a study by Zayat *et al.*[15] to determine the specificity of US-detected bone ero-

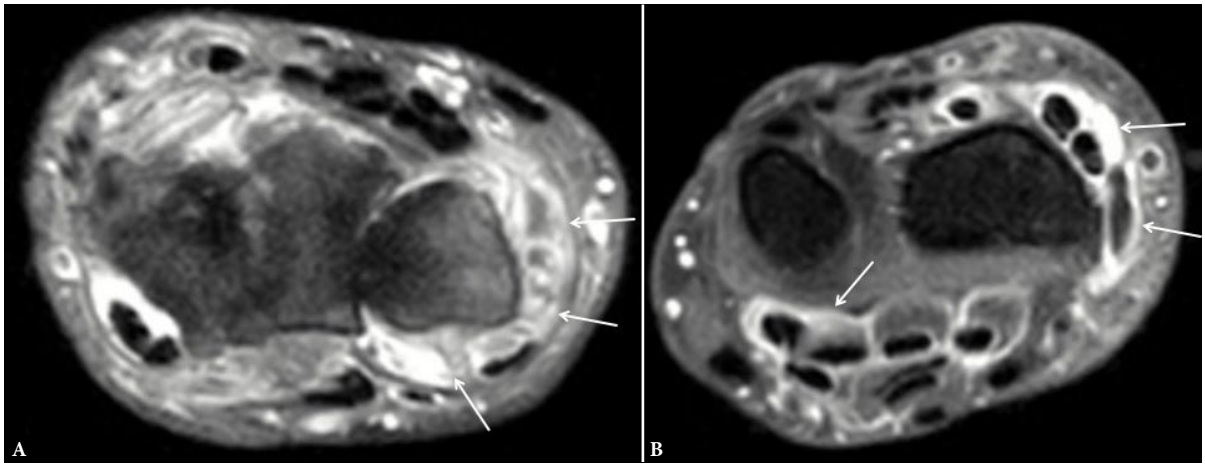

Fig. 6. *Axial post-contrast T1-weighted (T1W) fat-suppressed image of the distal radioulnar joint shows enhancing synovium (arrows in* **A***), suggesting synovitis along with enhancement of the flexor and extensor tendon sheaths (arrows in* **B***), consistent with tenosynovitis*

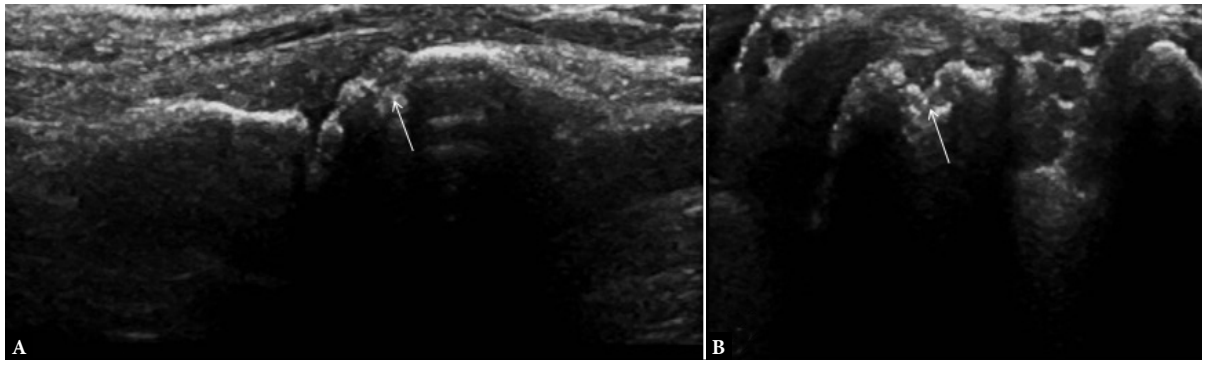

Fig. 7. *Erosions. Grayscale US images of the metacarpophalangeal joint in two orthogonal planes (***A** *and* **B***) show intraarticular discontinuity in the cortical bone surface (arrows)*

sions, the authors found that the presence of erosions is not specific for RA but larger erosions in the 2nd and 5th MCP, 5th MTP joints, and distal ulna were highly specific for and predictive of RA. Erosions of any size in the 5th MTP joint were both specific and sensitive for RA (specificity 85.4% and sensitivity 68.6%). Active inflammation associated with erosions can be detected with PD.

Potential pitfalls include normal cortical depressions, or pseudoerosions, commonly seen in the carpals and metacarpals (Fig. 8).

A recent semi-quantitative scoring system was developed for scoring erosions on US by the OMERACT task force[16] (Tab. 3).

On MRI, bone erosions are sharply marginated bone defects that are seen in at least two planes, with a cortical break visualized in at least one plane with low signal intensity on T1-weighted images[9,17] (Fig. 9). Histologically, they represent localized replacement of bone marrow fat by inflammatory cells adjacent to a cortical bone barrier[18]. The fluid or inflammatory tissue within the erosion appears hyperintense on T2-weighted images and may show enhancement on post-contrast T1-weighted images (Fig. 9).

Tab. 3. Scoring of bone erosions on US by the OMERACT task force

Grade 0	Intact cortical bone
Grade 1	Single small erosion (diameter: ≤2 mm)
Grade 2	Single large erosion (diameter: >2 mm) or 2 small erosions or 1 large and 1 small erosion
Grade 3	2 large erosions or ≥3 erosions, regardless of size

Aleo *et al.*[5] found that low-field MRI is probably more sensitive than US in the detection of erosions.

Bone marrow edema

Bone marrow edema appears as an ill-defined hyperintense area in the bone on T2FS or STIR (Fig. 10) sequences, and hypointense on T1W images showing post-contrast enhancement. The detection of bone marrow edema is unique to MRI. These lesions likely represent precursor lesions to subsequent bone erosion[19] and a risk factor for progression to structural joint damage. US is limited in its evaluation of internal bone structure.

Tenosynovitis

On US, tenosynovitis is defined as hypoechoic or anechoic thickened tissue, either with or without fluid within the tendon sheath, which is seen in two perpendicular planes and which may exhibit a Doppler signal[4] (Fig. 11). Tenosynovitis of the extensor carpi ulnaris (Fig. 12) is the most common, and represents an independent risk factor of erosive joint damage[10,20]. A study by Ohrndorf *et al.*[11]

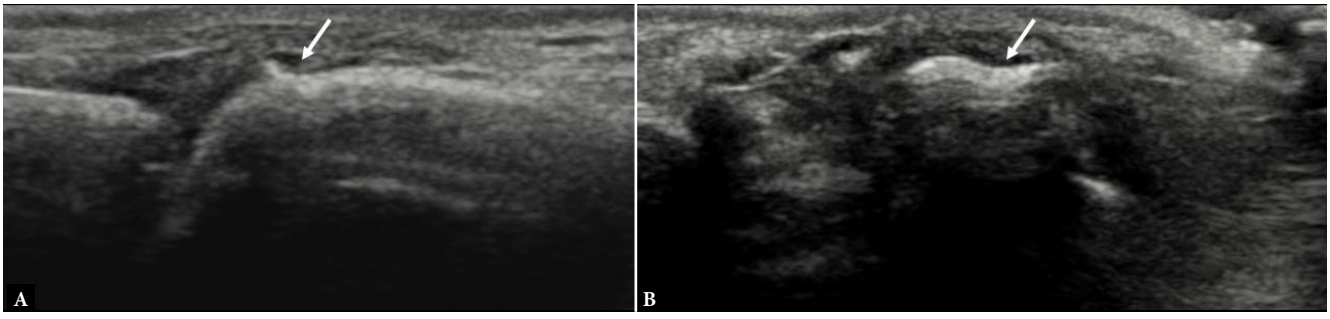

Fig. 8. *Grayscale US images of the 2nd metacarpal head in two orthogonal planes (***A** *and* **B***) show normal anatomical depression of dorsal cortical bone surface (arrows) mimicking erosion*

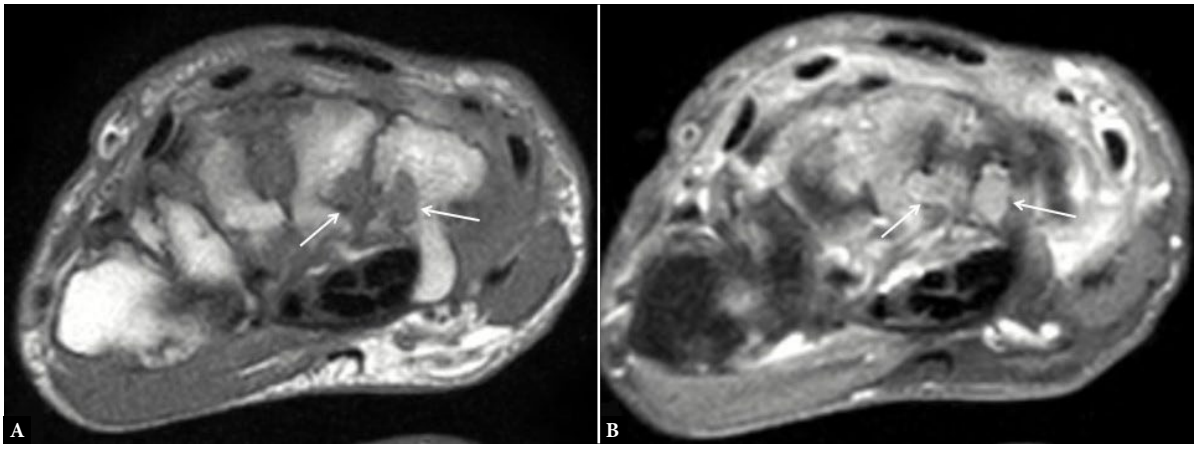

Fig. 9. *Erosions. Axial T1-W MR image of wrist joint reveals hypointense bony defects in the carpal bones (arrows in* **A***) showing enhancement on post-contrast T1-W fat-suppressed image (arrows in* **B***). Erosions in such locations can be missed on US*

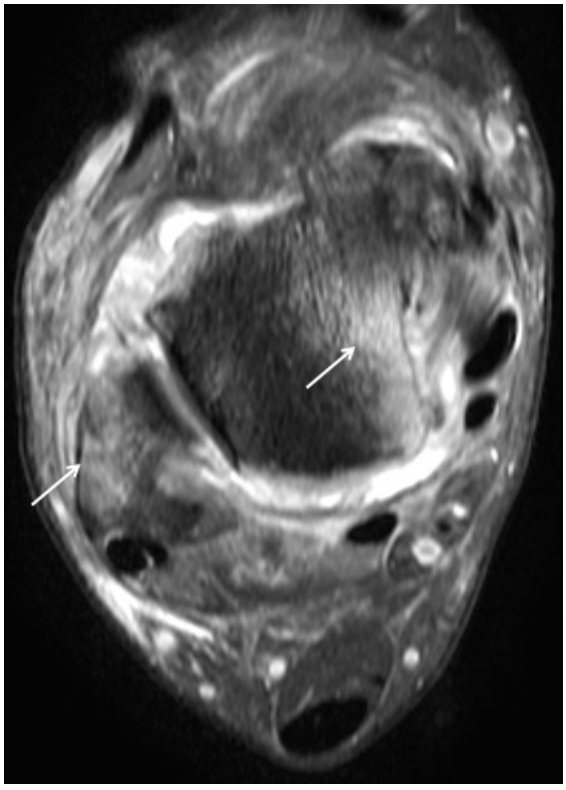

Fig. 10. *Bone marrow edema (BME). Axial STIR MR image of ankle joint shows patchy areas of hyperintense signal in the distal tibia and fibula (arrows). In this case, extensive BME was due to enthesitis*

found the specificity to detect tenosynovitis in grayscale and PD to be higher than the sensitivity.

On MRI, tenosynovitis appears as peritendinous fluid with thickening and enhancement of the tendon sheath (Fig. 13).

Bao *et al.*[21] concluded that US could be as sensitive and specific as contrast-enhanced MRI for the diagnosis of subclinical synovitis and tenosynovitis.

Synovitis leads to cartilage damage. Hyaline cartilage abnormalities can be detected by US, including cartilage thinning, blurring of margins, loss of clarity of the cartilaginous layer which may lose its normal homogeneously hypoechoic appearance, and irregularities of subchondral bone (Fig. 14).

Other manifestations of RA include rheumatoid nodules, tendinitis, carpal tunnel syndrome, and bursitis, which can be confidently diagnosed clinically and detected by both US and MRI. Enthesitis and sacroiliitis are uncommon manifestations in RA, and are best detected by MRI.

Spondyloarthropathies (SpA)

Spondyloarthropathies (SpA) are a heterogeneous group of inflammatory disorders including ankylosing spondylitis (AS), psoriatic arthritis, reactive arthritis, enteropathic arthritis, and undifferentiated spondyloarthritis. Enthesitis is a cardinal feature of SpA. Other features include synovitis, tenosynovitis, paratenonitis, and soft tissue edema. The main use of US in SpA is for the detection of enthesitis. Common sites for enthesitis are the insertion of the extensor tendons of fingers, Achilles tendon, plantar fascia, and quadriceps tendon.

On HRUS, enthesitis appears as heterogeneous hypoechogenicity of the enthesis, loss of normal fibrillar echotexture of the tendon inser-

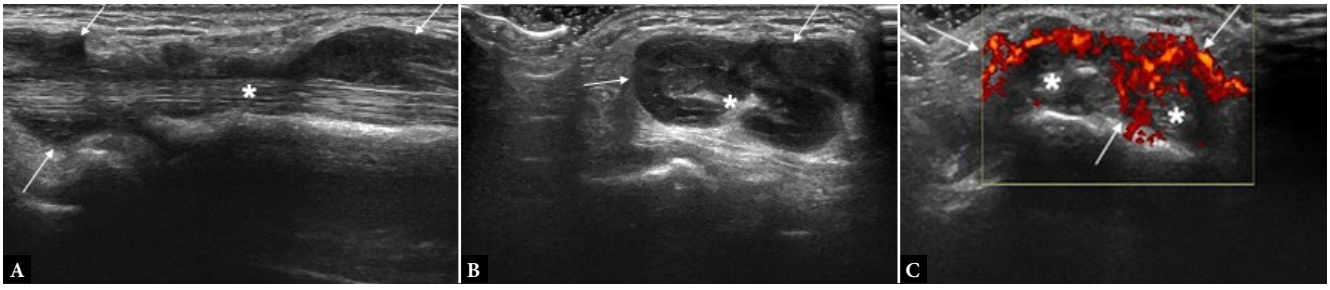

Fig. 11. *Tenosynovitis. Long- (***A***) and short-axis (***B***,***C***) US images of the 2nd extensor compartment tendons at wrist joint show circumferential hypoechoictenosynovial proliferation (arrows in* **A** *and* **B***) with significant power Doppler signal (arrow in* **C***) suggestive of active tenosynovitis, in a known case of RA*

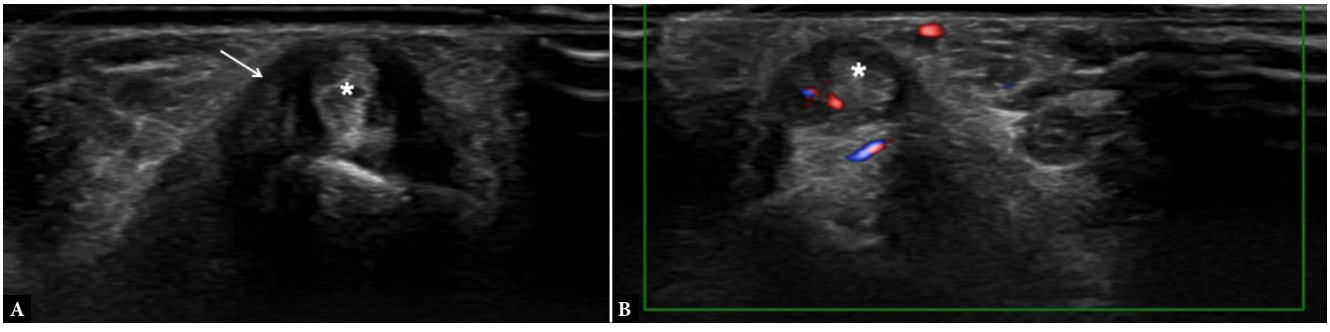

Fig. 12. *Extensor carpi ulnaris (ECU) tenosynovitis. Short-axis grayscale (***A***) and power Doppler (***B***) US of the ECU (asterisks) shows sheath thickening (arrow in* **A***) with power Doppler signal keeping with tenosynovitis, in a patient with RA*

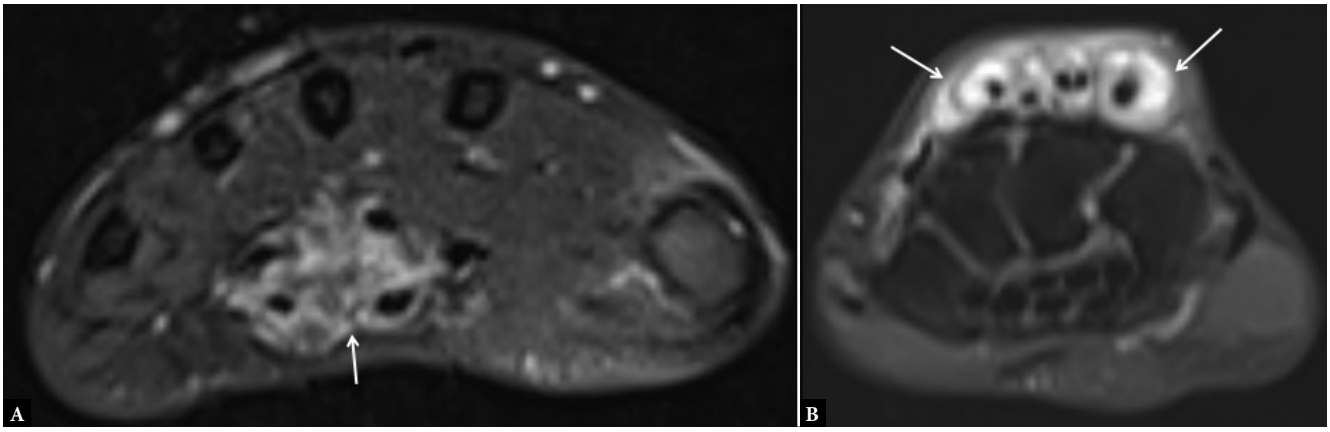

Fig. 13. *Tenosynovitis. Axial proton density fat-suppressed images of different patients (A and B) show tenosynovial proliferation and edema of flexor (arrow in* **A***) and extensor (arrow in* **B***) tendons*

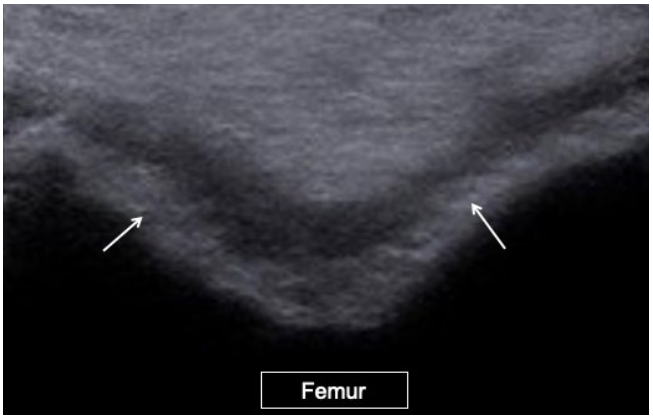

Fig. 14. *Cartilage damage. Short-axis US image of the knee joint at the level of trochlea shows blurring of cartilage margins, loss of clarity of the cartilaginous layer, and loss of its normal homogeneously hypoechoic appearance*

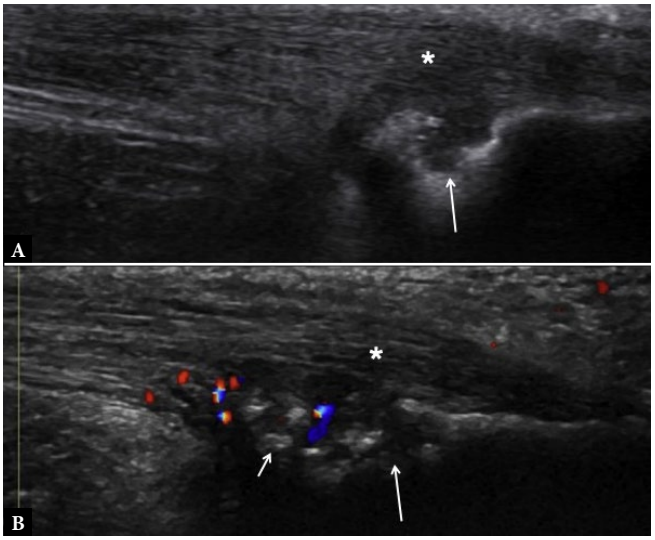

Fig. 15. *Enthesitis. Long-axis US images of Achilles tendon show loss of normal fibrillar echotexture and decreased echogenicity of the tendon insertion (asterisks), punctate calcific foci (small arrow in* **B***), erosions of subentheseal bone (large arrows in* **A** *and* **B***) and power Doppler signal at enthesis as seen in* **B**

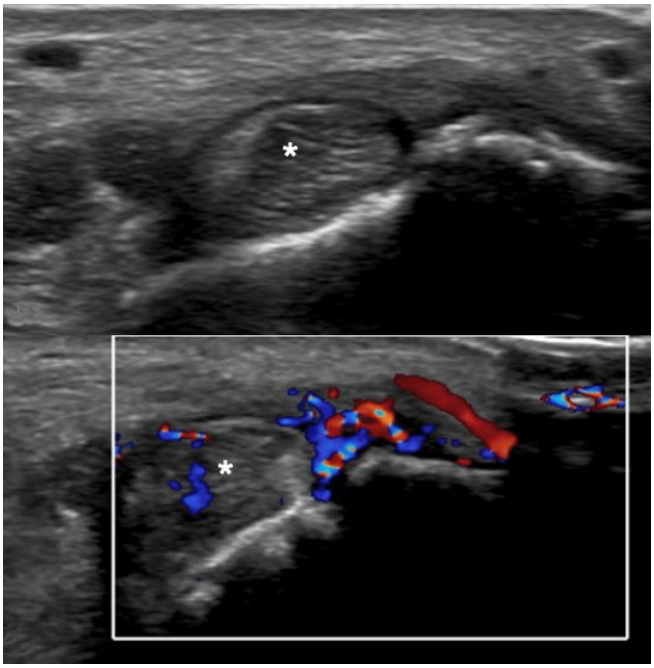

Fig. 16. *Enthesitis. Short-axis grayscale (***A***) and power Doppler (***B***) US images of tibialis posterior tendon (asterisks) show intra-tendinous and peritendinous thickening and power Doppler signal*

tion, intratendinous hypoechoic areas, punctate calcific foci, blurring of tendon margins, thickening of the insertion site of tendon, irregularities, and erosions of subentheseal bone, and perientheseal swelling (Fig. 15). Perientheseal diffusion of inflammatory fluid noted on imaging has been reported to be a characteristic finding of SpA and cause perientheseal swelling[22]. Multiple and irregular enthesophytes and calcific deposits are more specific for SpA-related enthesitis[22]. PDUS can show an increased signal in active inflammation of the enthesis and can be used to assess treatment response (Fig. 16).

Dactylitis, a feature of psoriatic arthritis, is associated with flexor tenosynovitis, diffuse extensor paratenonitis, soft tissue thickening, or edema (Fig. 17). Palmar plate inflammation, digital enthesitis, and collateral ligament enthesitis are other features that may be present in psoriatic arthritis[23].

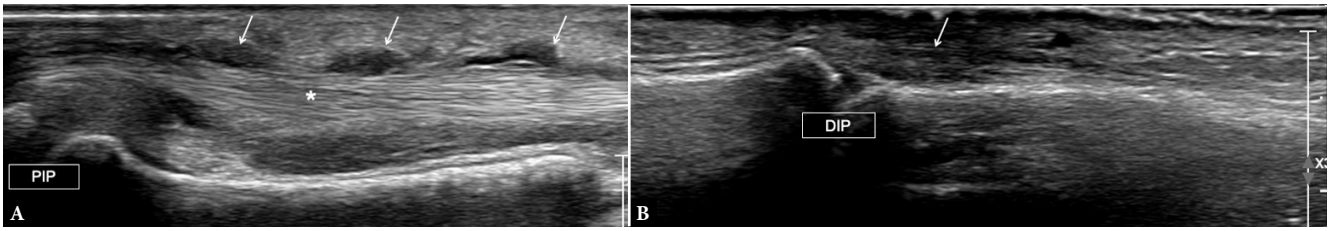

Fig. 17. *Dactylitis. Long-axis US image of flexor tendons (***A***) and extensor tendon (***B***) of the fingers of the same patient show tenosynovial proliferation (arrows in A) around flexor tendons (asterisk), representing tenosynovitis. There is thickening of the extensor tendon (arrow in* **B***) at its insertion to the distal phalanx. PIP – proximal interphalangeal joint; DIP – distal interphalangeal joint*

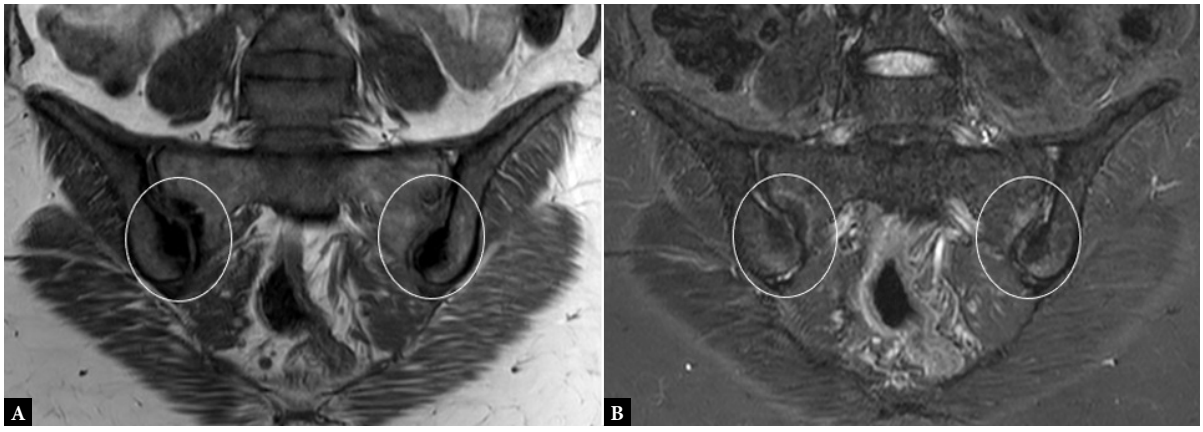

Fig. 18. *Sacroiliitis. Coronal oblique T1-W (***A***) and STIR (***B***) MR images of sacroiliac joints show bilateral symmetrical periarticular BME (hyperintensity within the circles in* **B***) with areas of sclerosis (hypointensity within circles in* **A***). There is a mild reduction in joint spaces and irregularity of articular marginsv*

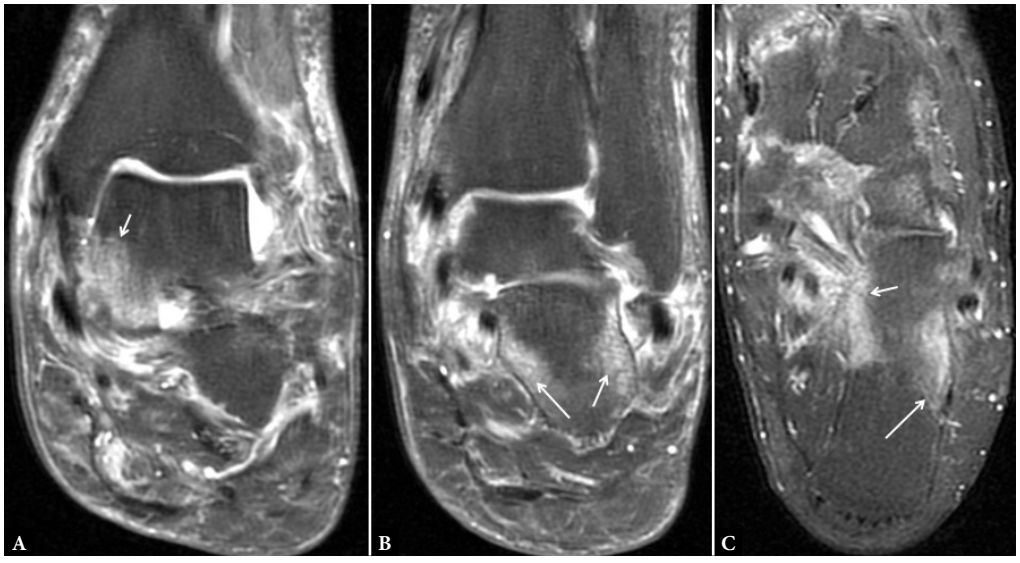

Fig. 19. *Enthesitis. MR proton density fat-suppressed coronal (***A** *and* **B***) and axial images of the ankle show extensive marrow edema (hyperintensity) at the attachment sites of ligaments (small arrows in* **A** *and* **C***); retinaculum (arrows in* **B***) and fascia (long arrow in* **C***)*

MRI studies of patients with dactylitis have shown increased signals at the palmar plate.

The role of MRI in SpA is to diagnose active inflammatory lesions, monitor disease activity, and diagnose complications, such as cartilage damage, tendon tears, and osteonecrosis. MRI is primarily used for the imaging of sacroiliac joints in axial SpA to detect sacroiliitis (Fig. 18).

On MRI, an abnormal enthesis is hyperintense on fluid-sensitive sequences and hypointense on T1-weighted images. The bony part of an enthesis may show significant bone marrow edema (Fig. 19). On post-contrast images, both fibrous and bony parts of the enthesis show enhancement. When synovium is present in an adjacent bursa or joint, it can also appear inflamed. Enthesophytes can also be detected at the bursal site[9]. The presence of bone marrow edema indicates inflammatory enthesitis. MRI is very sensitive in detecting

active inflammatory enthesitis, even though in a systematic review, Aleo *et al*. found that US was more sensitive to detect early changes of enthesopathy than MRI[5] .

Osteoarthritis (OA)

Osteoarthritis is the most widespread form of arthritis. The most commonly affected joints are the weight-bearing type, or the ones used repetitively – the hip, knee, foot, and hand. Radiography is the primary imaging modality to evaluate OA. Radiographic features include marginal osteophytes, asymmetrical joint space narrowing, subchondral sclerosis, and subchondral cysts (Fig. 20). Joint space narrowing is an indirect surrogate marker to assess articular cartilage loss on radiographs. Increasingly, HRUS and MRI are being utilized for the evaluation of soft tissues in the OA joint.

HRUS can detect alterations in cartilage, marginal osteophytes, effusion, synovitis, and bursal distention.

On US, normal cartilage appears as a homogeneous hypoechoic to anechoic structure of uniform thickness. In OA, the cartilage may appear heterogeneous, with uneven thickness and fuzzy contours. Osteophytes appear as echogenic elevated bony projections near the articular margin (Fig. 21). Several studies have demonstrated the presence of grayscale synovitis in hand OA[24].

In the knee joint, HRUS is more sensitive than radiography to depict tibiofemoral osteophytes[25]. Part of normal knee menisci can be seen on US, appearing as triangular echogenic structures lying within the confines of the bony margins. HRUS is able to identify meniscal injury in some instances which can be associated with other structural tissue damage in the knee and can increase the risk of progression to OA (Fig. 22)[26].

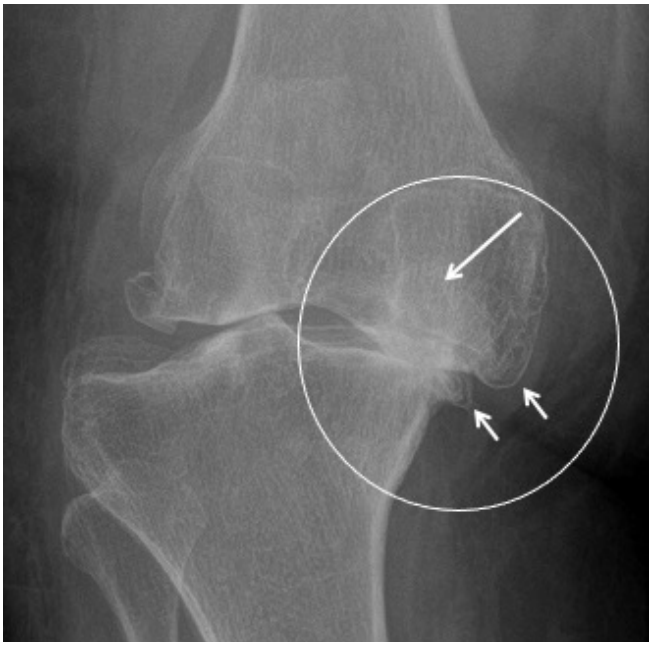

Fig. 20. *Severe osteoarthritis (OA). AP radiograph of the right knee shows marginal osteophytes (small arrows), medial joint space narrowing (circle), subchondral sclerosis, and subchondral cysts (long arrow)*

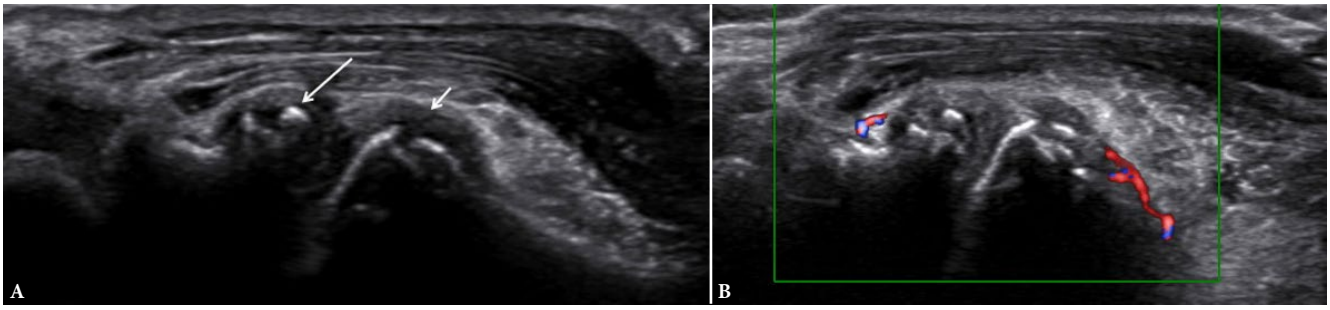

Fig. 21. *Osteoarthritis (OA). Long-axis grayscale (***A***) and power Doppler (***B***) US images of the 1st carpometacarpal and joint show osteophytes (long arrow in* **A***) along with synovial and capsular thickening (short arrow in* **A***). There is a power Doppler signal in the thickened synovium as seen in B. The 1st carpometacarpal joint is one of the joints involved early on in OA*

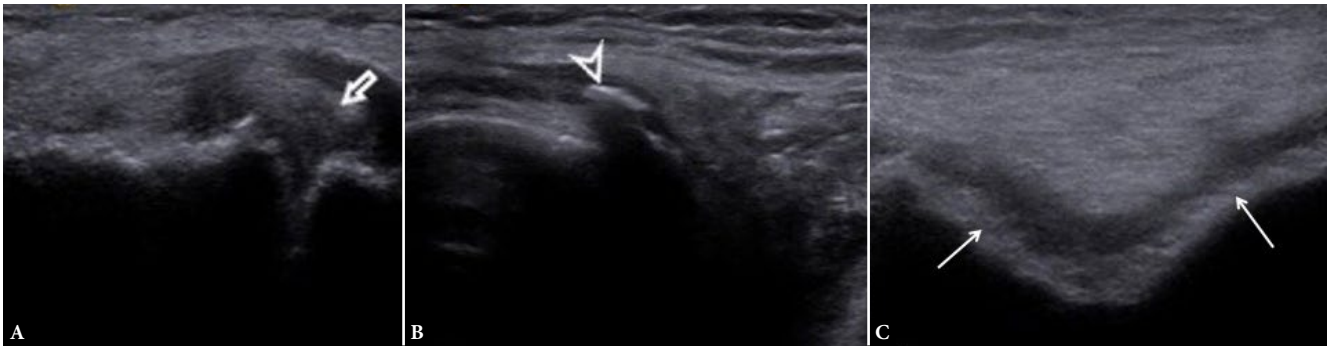

Fig. 22. *Osteoarthritis (OA). Long-axis US images of the knee joint show meniscal extrusion (arrow in* **A***), osteophyte (arrowhead in* **B***), and cartilage damage of trochlea (arrows in* **C***), cartilage appears heterogeneous, with uneven thickness and fuzzy contours*

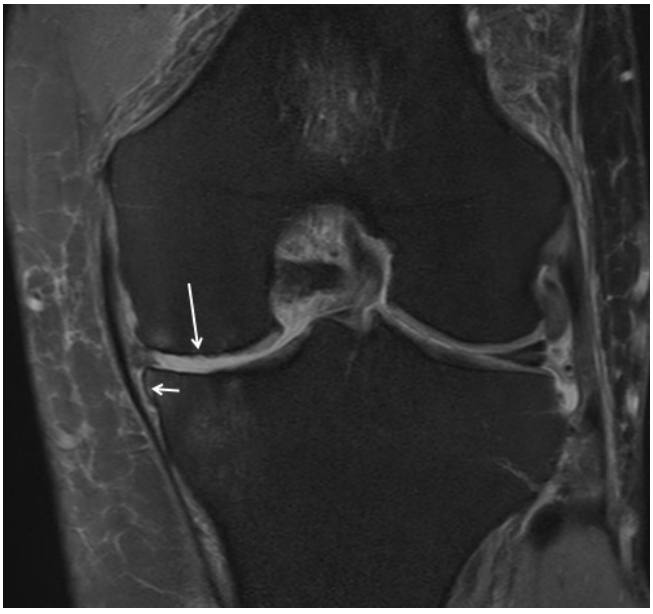

Fig. 23. *Osteoarthritis (OA): MR proton density fat-suppressed coronal image shows cartilage damage with cortical irregularity (long arrow) and osteophyte (small arrow). There is also tear of medial meniscus*

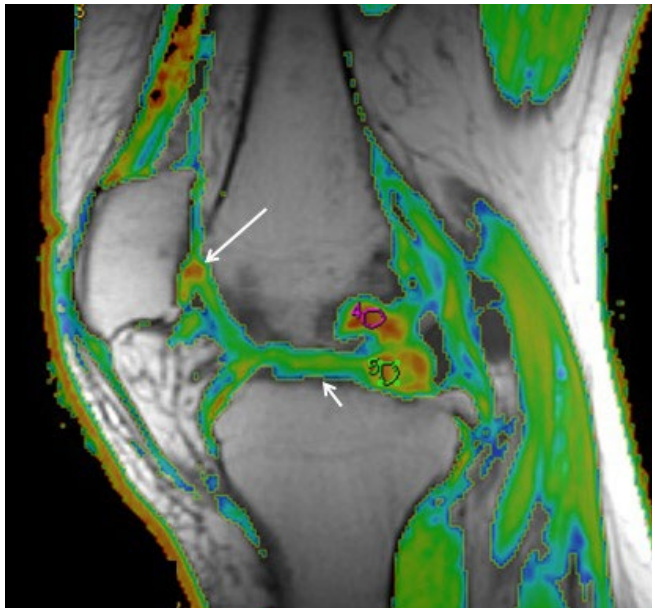

Fig. 24. *Cartilage imaging. Sagittal T2 mapping shows different color shades of the cartilage based on the diffusing fluid signal. Color shade towards red indicates cartilage damage(long arrow) and shade towards blue indicates healthy cartilage (small arrow)*

US has limitations in visualizing joint tissues due to the limited acoustic window which may be further limited by the presence of large osteophytes. Also, it cannot assess the bone changes like subchondral cysts, sclerosis, and bone marrow alterations which are all common features of OA.

US is comparative to MRI in the assessment of osteophytes, bone erosions, and synovitis, in erosive and hand nodal OA[24].

MRI has the advantage of visualizing bone, intraarticular tissues, cartilage, ligaments, menisci, and internal bone structure (Fig. 23).

Recent developments in MRI, including high-resolution three-dimensional sequences, allow the quantification of articular cartilage. Quantitative measurements of cartilage volume and thickness change are used in studies to evaluate different treatment outcomes.

Techniques that analyze cartilage composition like T2-mapping, which assesses collagen and water content (Fig. 24), and delayed gadolinium-enhanced MRI of cartilage (dGEMRIC), which assesses glycosaminoglycan content, have been developed. These are being investigated for the early diagnosis of OA, monitoring treatment response, and possible intervention at an early reversible stage[25].

Crystal-induced arthropathies: gout and pseudogout

Gout is an inflammatory arthritis associated with hyperuricemia. It is characterized by the deposition of monosodium urate crystals in the articular and extraarticular tissues, synovitis, and bone erosions.

HRUS can accurately assess crystal deposition in various tissues, including the synovial membrane, cartilage, tendons, bursae, and soft tissues. In the early stages, US reveals characteristic features such as effusion and echogenic synovitis[24]. Hyperechoic spots representing crystals can be observed in the joint and periarticular tissues (Fig. 25, Fig. 26). PD US can detect increased color signals

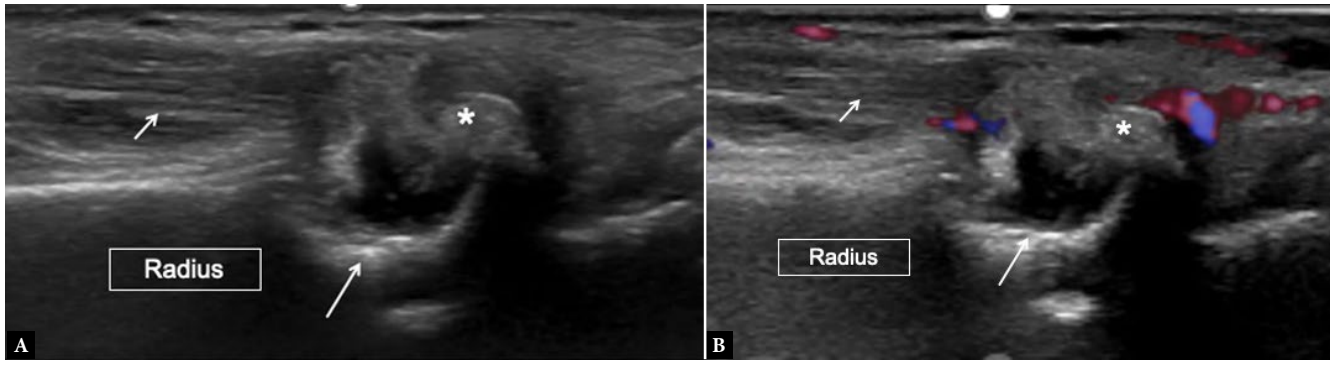

Fig. 25. *Gout. Long-axis grayscale (**A**) and power Doppler (**B**) US image at the wrist joint shows large overhanging erosion in the radius (long arrows) adjacent to extensor digitorum tendon (short arrows). There is a large echogenic tophus overlying the erosion (asterisks) with surrounding power Doppler signal (**B**)*

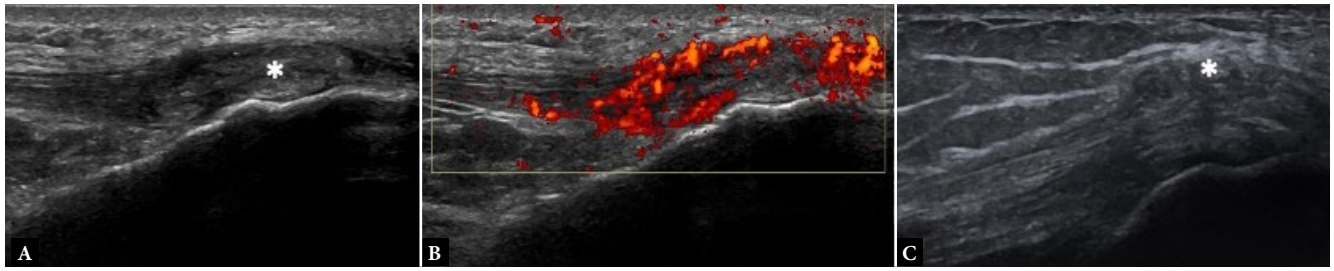

Fig. 26. *Gout. US intratendinous crystal.* **A.** *Deposition of monosodium urate crystals in the patellar tendon (asterisk);* **B.** *with Power Doppler signal suggestive of active inflammation.* **C.** *Long-axis view of triceps tendon near its insertion, with a tophaceous deposit (asterisk) seen as inhomogeneous echogenicity with loss of normal fibrillar pattern*

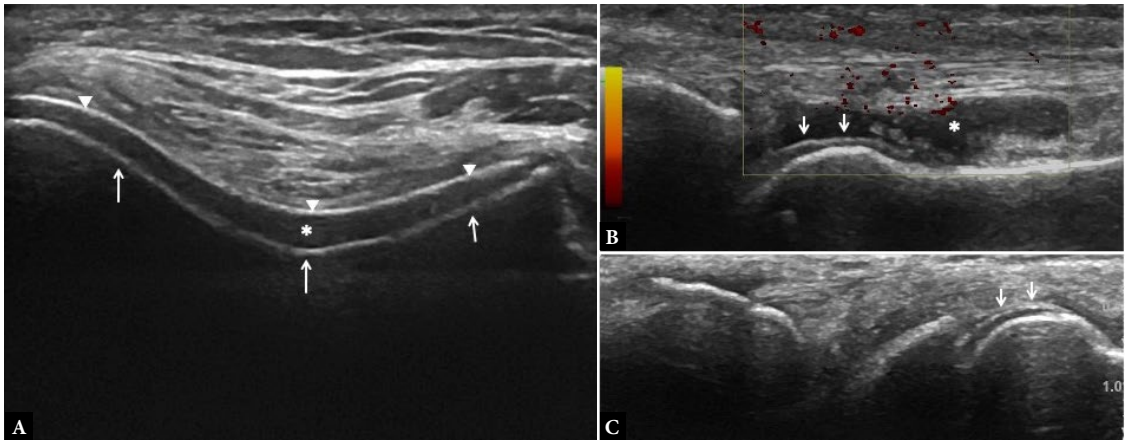

Fig. 27. *Gout.* **A.** *Transverse US image of the suprapatellar knee joint demonstrates two parallel hyperechoic contours on either side of the hypoechoic hyaline cartilage (asterisk). The deep echogenic contour (long arrows) represents the femoral cortex, while the superficial echogenic contour (arrowheads) represents monosodium urate crystals accumulating on the surface of the hypoechoic hyaline cartilage (asterisk). Long-axis US image of metatarsophalangeal joint (***B***) and wrist joint (***C***) with the double contour sign (arrows) around hyaline cartilage. Note the anechoic synovial effusion with hyperechoic crystal deposits (snow-storm appearance) in the first metatarsophalangeal joint without any power Doppler signal (asterisk in* **B***)*

in the inflamed synovial tissue (Fig. 25, Fig. 26). Gouty tophi appear as heterogeneous structures with a peripheral hypoechoic rim. Monosodium urate crystals deposit on the superficial surface of the hyaline cartilage, generating an echogenic line over subjacent hypoechoic cartilage and parallel echogenic bone cortex, giving the appearance of a double contour known as the "double contour" sign[27] (Fig. 27).

Studies have shown that US correlates well with MRI in the detection of tophi[28]. Erosions are more easily detected on US than on radiography[29]. Gouty erosions can be intraarticular or extraarticular. There is evidence that reduction is US features of gout parallels the reduction in serum urate levels[24].

MRI is helpful in the assessment of the extent of joint, tendon, and bursal involvement, and in diagnosing complications, including tendon tears. On MRI, tophi are low signal on T1-weighted MRI and mostly intermediate signal on T2-weighted MRI, and can show enhancement on post-contrast images. Low signal foci on T2-weighted images most likely represent calcifications (Fig. 28).

In pseudogout, calcium pyrophosphate crystals deposit (CPPD) as echogenic foci of different sizes or as a linear band within the substance of the hyaline cartilage. These findings have a moderate sensitivity but an excellent specificity to differentiate between gout and pseudogout.

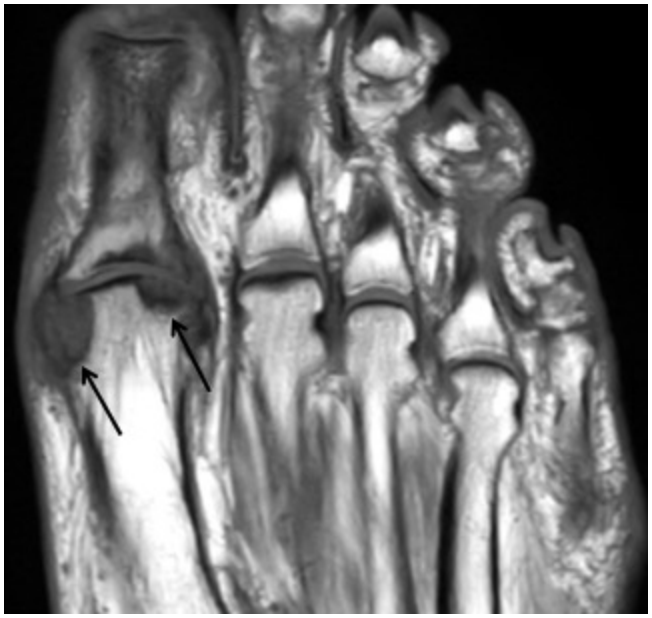

Fig. 28. *Gout: Coronal T1-W MR image of the foot shows large hypointense erosions in the head of the 1st metatarsal (black arrows) with adjacent hypointense tophi. There is also a large hypointense tophus over the base of the 5th metatarsal (white arrow). Note the characteristic clearly demarcated erosion*

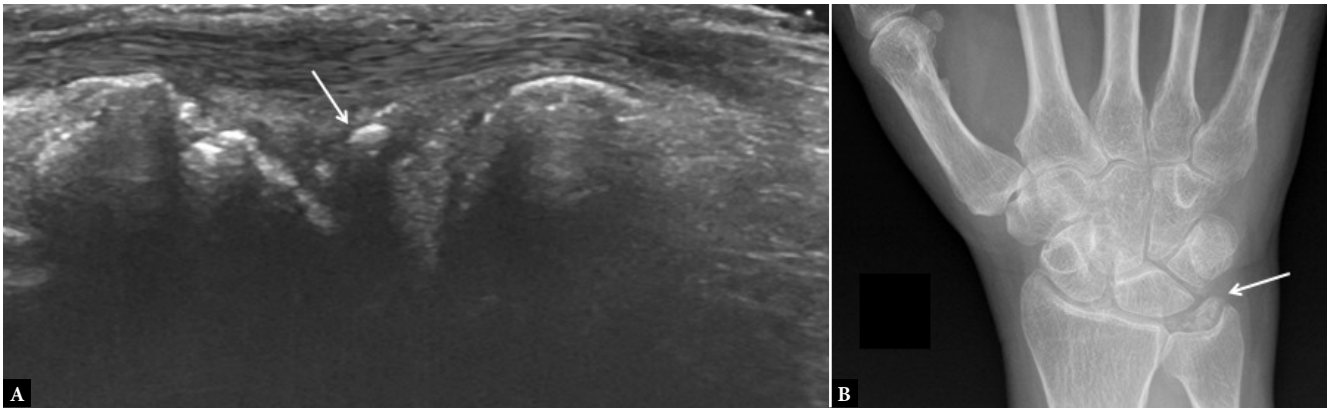

Fig. 29. *Calcium pyrophosphate crystals deposit (CPPD) disease: long-axis US image of medial wrist joint shows nodular hyperechoic deposit in the region of triangular fibrocartilage (arrow in* **A***) which is seen as a calcific opacity in radiograph (arrow in* **B***)*

In CPPD disease, echogenic spots may be seen at the fibrocartilage sites, such as the menisci, and triangular fibrocartilage. In the tendons, crystals can appear as linear hyperechoic areas and in the synovial cavity as hyperechoic dots of variable sizes (Fig. 29).

Calcifications in the Achilles tendon are highly specific for CPPD disease and US has shown a high agreement with radiography in the detection of entheseal calcifications and enthesophytosis in this disease[22].

Recent advances

DCE-MRI allows measurement of tissue perfusion and has clinical applications in the assessment for synovial changes to help guide diagnosis, monitor disease activity, and evaluate treatment efficacy. For example, reduction in synovial perfusion has been shown to be a more sensitive indicator of treatment response than synovial volume[30].

Contrast-enhanced US (CEUS) utilizes microbubble-based contrast agents to intensify the Doppler signal in small vessels and help identify synovitis[31]. It can thus aid in determining disease activity. The use of CEUS is also being investigated in inflammatory back pain and sacroiliitis. Microvascular imaging is another technique that enhances low-flow signals and can be used in the detection of active synovitis[31]. US elastography measures the stiffness of tissues qualitatively (strain elastography) and quantitatively (shear wave elastography)[32]. In inflammation and even in osteoarthritis, there are pathological alterations in muscles and tendons. For example, tendons become softer with reduced elasticity. Further research is needed to evaluate the diagnostic capabilities and potential clinical application of these techniques in various musculoskeletal conditions.

Dual-energy CT (DECT) employs simultaneous scanning using two energy sources of different X-ray energy levels (80 kV and 140 kV). Evaluation of the different attenuations of the scanned object allows analysis of the chemical composition of materials, which can be color-coded for visualization and then measured. By analyzing the differences in X-ray absorption between uric acid crystals and surrounding tissues, DECT can detect the presence and distribution of urate crystals in gout (Fig. 30). It can assess the volume of crystals and help in differentiating gout from other crystal deposition diseases.

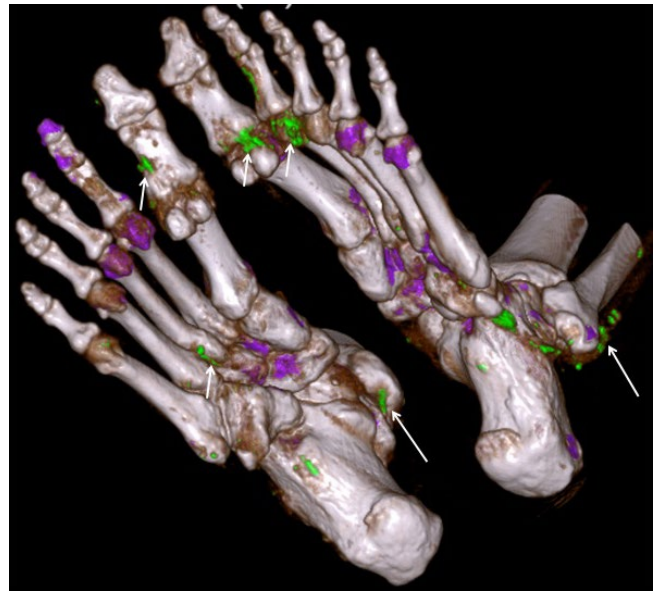

Fig. 30. *Dual-energy CT (DECT) in gout: 3D reconstructed image of DECT of both feet in a patient with gout shows green color-coded crystal aggregates around the joints (small arrows) and along the tendons (long arrows)*

Conclusions

HRUS and MRI are valuable imaging modalities in rheumatology for assessing musculoskeletal structures and detecting inflammatory and structural changes, with good diagnostic performance. HRUS is low-cost, easily accessible, portable, and provides real-time imaging with high resolution. It enables detailed evaluation of superficial joints, tendons, cartilage, and entheses, providing information on synovial hypertrophy, tenosynovitis, vascularity, effusion, and bone erosions for early detection and monitoring of disease activity in various rheumatic conditions. PD US improves US sensitivity for diagnosing active inflammation.

MRI provides superior soft tissue contrast and allows comprehensive assessment of intraarticular structures, bone, and detection of bone marrow edema. It assesses disease activity, structural lesions, and complications. Advanced MRI techniques aid in early diagnosis, treatment monitoring, and intervention for various rheumatic diseases.

Both modalities offer complementary information and can be used in combination to provide a comprehensive assessment of disease activity, treatment response, and prognostic evaluation, increasing diagnostic accuracy and improving patient outcomes. Ongoing advancements in imaging technology will further refine these modalities, enhancing their clinical utility.

Conflict of interest

The authors do not report any financial or personal connections with other persons or organizations which might negatively affect the contents of this publication and/or claim authorship rights to this publication.

Author contributions

Original concept of study: GG. Writing of manuscript: AKS, GG. Analysis and interpretation of data: SK, GG. Final approval of manuscript: GG. Collection, recording and/or compilation of data: GG. Critical review of manuscript: GG.

References

1. Theis KA, Murphy LB, Guglielmo D, Boring MA, Okoro CA, Duca LM *et al.*: Prevalence of arthritis and arthritis-attributable activity limitation – United States, 2016–2018. MMWR Morb Mortal Wkly Rep 2021; 70: 1401–1407. doi: http://dx.doi.org/10.15585/mmwr.mm7040a2.
2. Hootman JM, Helmick CG, Barbour KE, Theis KA, Boring MA: Updated projected prevalence of self-reported doctor-diagnosed arthritis and arthritis-attributable activity limitation among U.S. adults, 2015–2040. Arthritis Rheumatol 2016; 68: 1582–1587. doi: 10.1002/art.39692.
3. Taljanovic MS, Melville DM, Gimber LH, Scalcione LR, Miller MD, Kwoh CK *et al.*: High-resolution US of rheumatologic diseases. Radiographics 2015; 35: 2026–2048. doi: 10.1148/rg.2015140250.
4. Wakefield RJ, Balint PV, Szkudlarek M, Filippucci E, Backhaus M, D'Agostino MA *et al.*: Musculoskeletal US including definitions for ultrasonographic pathology. J Rheumatol 2005; 32: 2485–2487.
5. Aleo E, Barbieri F, Sconfienza L, Zampogna G, Garlaschi G, Cimmino MA: US versus low-field magnetic resonance imaging in rheumatic diseases: a systematic literature review. Clin Exp Rheumatol 2014; 32: S91–98.
6. Szkudlarek M, Court-Payen M, Jacobsen S, Klarlund M, Thomsen HS, Østergaard M: Interobserver agreement in ultrasonography of the finger and toe joints in rheumatoid arthritis. Arthritis Rheum 2003; 48: 955–962. doi: 10.1002/art.10877.
7. D'Agostino MA, Terslev L, Aegerter P, Backhaus M, Balint P, Bruyn GA *et al.*: Scoring ultrasound synovitis in rheumatoid arthritis: a EULAR-OMERACT US taskforce – Part 1: definition and development of a standardized, consensus-based scoring system. RMD Open 2017; 3: e000428. doi: 10.1136/rmdopen-2016-000428.
8. Terslev L, Naredo E, Aegerter P, Wakefield RJ, Backhaus M, Balint P *et al.*: Scoring ultrasound synovitis in rheumatoid arthritis: a EULAR-OMERACT US taskforce – Part 2: reliability and application to multiple joints of a standardized consensus-based scoring system. RMD Open 2017; 3: e000427. doi: 10.1136/rmdopen-2016-000427.
9. Sudoł-Szopińska I, Jurik AG, Eshed I, Lennart J, Grainger A, Østergaard M *et al.*: Recommendations of the ESSR arthritis subcommittee for the use of magnetic resonance imaging in musculoskeletal rheumatic diseases. Semin Musculoskelet Radiol 2015; 19: 396–411. doi: 10.1055/s-0035-1564696.
10. Rowbotham EL, Grainger AJ: Rheumatoid arthritis: ultrasound versus MRI. AJR Am J Roentgenol 2011; 197: 541–546. doi: 10.2214/ajr.11.6798.
11. Ohrndorf S, Boer AC, Boeters DM, Ten Brinck RM, Burmester GR, Kortekaas MC *et al.*: Do musculoskeletal US and magnetic resonance imaging identify synovitis and tenosynovitis at the same joints and tendons? A comparative study in early inflammatory arthritis and clinically suspect arthralgia. Arthritis Res Ther 2019; 21: 59. doi: 10.1186/s13075-019-1824-z.
12. Takase-Minegishi K, Horita N, Kobayashi K, Yoshimi R, Kirino Y, Ohno S *et al.*: Diagnostic test accuracy of ultrasonography for synovitis in rheumatoid arthritis: systematic review and meta-analysis. Rheumatology (Oxford) 2018, 57: 49–58. doi: 10.1093/rheumatology/kex036.
13. Fritz J: Magnetic resonance imaging versus ultrasonography for the diagnosis of synovitis in rheumatoid arthritis. Rheumatology 2018; 57: 5–7. https://doi.org/10.1093/rheumatology/kex237.
14. Wakefield RJ, Gibbon WW, Conaghan PG, O'Connor P, McGonagle D, Pease C *et al.*: The value of sonography in the detection of bone erosions in patients with rheumatoid arthritis: A comparison with conventional radiography. Arthritis Rheum 2000, 43, 2762–2770. doi: 10.1002/1529-0131(200012)43:12<2762::AID-ANR16>3.0.CO;2-#.
15. Zayat AS, Ellegaard K, Conaghan PG, Terslev L, Hensor EM, Freeston JE *et al.*: The specificity of US-detected bone erosions for rheumatoid arthritis. Ann Rheum Dis 2015; 74: 897–903. doi: 10.1136/annrheumdis-2013-204864.
16. Mandl P, Gessl I, Filippou G, Sirotti S, Terslev L, Pineda C *et al.*: POS0161 An US scoring system based on the size and number of erosions is reliable in rheumatoid arthritis. Ann Rheum Dis 2023; 82: 303.
17. Østergaard M, Peterfy C, Conaghan P, McQueen F, Bird P, Ejbjerg B *et al.*: OMERACT Rheumatoid Arthritis Magnetic Resonance Imaging Studies. Core set of MRI acquisitions, joint pathology definitions, and the OMERACT RAMRI scoring system. J Rheumatol 2003; 30: 1385–1386.
18. Jimenez-Boj E, Nöbauer-Huhmann I, Hanslik-Schnabel B, Dorotka R, Wanivenhaus AH, Kainberger F *et al.*: Bone erosions and bone marrow edema as defined by magnetic resonance imaging reflect true bone marrow inflammation in rheumatoid arthritis. Arthr Rheum 2007; 56: 1118–1124. https://doi.org/10.1002/art.22496.
19. Isbel M, Paramalingam S, Conaghan PG, Keen HI: An update on imaging in rheumatoid arthritis. Curr Treat Options Rheum 2020; 6: 370–381.
20. Lillegraven S, Bøyesen P, Hammer HB, Østergaard M, Uhlig T, Sesseng S *et al.*: Tenosynovitis of theextensor carpi ulnaris tendon predicts erosive progression in earlyrheumatoid arthritis. Ann Rheum Dis 2011; 70: 2049–2050. doi: 10.1136/ard.2011.151316.
21. Bao Z, Zhao Y, Chen S, Chen X, Xu X, Wei L *et al.*: . US versus contrast-enhanced magnetic resonance imaging for subclinical synovitis and tenosynovitis: a diagnostic performance study. Clinics (Sao Paulo) 2020; 75: e1500. doi: 10.6061/clinics/2020/e1500.
22. Falsetti P, Acciai C, Lenzi L, Frediani B: Ultrasound of enthesopathy in rheumatic diseases. Mod Rheumatol 2009; 19: 103–113. doi: 10.1007/s10165-008-0129-x.
23. Kaeley GS, Bakewell C, Deodhar A: The importance of ultrasound in identifying and differentiating patients with early inflammatory arthritis: a narrative review. Arthritis Res Ther 2020; 22: 1. doi: 10.1186/s13075-019-2050-4.
24. Ruta S, Reginato AM, Pineda C, Gutierrez M, Pan-American League Against Rheumatisms (PANLAR) US Study Group: General applications of ultrasound in rheumatology: why we need it in our daily practice. J Clin Rheumatol 2015; 21: 133–143. doi: 10.1097/RHU.0000000000000230.
25. Roemer FW, Demehri S, Omoumi P, Link TM, Kijowski R, Saarakkala S *et al.*: State of the art: imaging of osteoarthritis-revisited 2020. Radiology 2020; 296: 5–21. doi: 10.1148/radiol.2020192498.
26. Kaeley GS, Ramrattan LA, Ranganath VK: Sonography of common rheumatic diseases. Indian J Rheumatol 2018; 13: S48–S56. doi: 10.4103/0973-3698.238202.
27. Jain M, Samuels J: Musculoskeletal ultrasound in the diagnosis of rheumatic disease. Bull NYU Hosp Jt Dis 2010; 68: 183–190.
28. Perez-Ruiz F, Martin I, Canteli B: Ultrasonographic measurement of tophi as an outcome measure for chronic gout. J Rheumatol 2007; 34: 1888–1893.
29. Wright SA, Filippucci E, McVeigh C, Grey A, McCarron M, Grassi W *et al.*: High-resolution ultrasonography of the first metatarsal phalangeal joint in gout: a controlled study. Ann Rheum Dis 2007; 66: 859–864. doi: 10.1136/ard.2006.062802.
30. Eshed I, Hermann KGA: MRI in imaging of rheumatic diseases: an overview for clinicians. Clin Exp Rheumatol 2018; 36 Suppl 114: 10–15.
31. Sakellariou G, Giovannini I, Grignaschi S, Zabotti A, Iagnocco A: New developments in ultrasound in rheumatology: innovative tools and promising applications. Clin Exp Rheumatol 2021; 39: 413–421. doi: 10.55563/clinexprheumatol/5tf1kq.
32. Taljanovic MS, Gimber LH, Becker GW, Latt LD, Klauser AS, Melville DM *et al.*: Shear-wave elastography: basic physics and musculoskeletal applications. Radiographics 2017; 37: 855–870. doi: 10.1148/rg.2017160116.